Supplementary Materials:

Postnatal Sustentacular Cells as Chromaffin Progenitors and Tumor Cells of Origin in VHL-Related Paragangliomas

Petra Bullova[† 1], Peng Cui[† 1], Maria Arceo[1], Jiacheng Zhu[1], Wenyu Li[1], Valentin P[1], Monika Plescher[1], Katerina Stripling[1, 2], Christian Santangeli[1], Maria Eleni Kastriti[3], Catharina Larsson[1], C. Christofer Juhlin[1], Michael Mints[1*] and Susanne Schlisio[1*]

*Corresponding authors: Michael Mints michael.mints@ki.se, and Susanne Schlisio susanne.schlisio@ki.se.

This PDF file includes:

Supplementary Materials and Methods

Tamoxifen-induced lineage tracing, EdU administration and tissue collection

Time-mating groups were started in the afternoon. The day of birth was considered as P0. For postnatal induction of *Cre* expression (*Sox10*^{CreERT2}), oral gavage of the nursing female mouse was performed daily with 2 mg tamoxifen (Sigma-Aldrich, #T5648, dissolved in corn oil [Sigma-Aldrich, #C9267]) for 5 days (P0-4).

For postnatal tissue isolation, 5-days old (P5) mice were euthanized by decapitation. Mice older than 13 days, for example the 14-days old (P14) and 90-days old (P90) mice, were euthanized by carbon dioxide inhalation. After euthanasia, bilateral adrenal glands were immediately dissected out. The right adrenal glands were placed in ice-cold 1× PBS, while the left ones were snap-frozen on dry ice. To assess proliferation in adrenal glands, some of the animals were administered with 5-ethyl-2-deoxyuridine (EdU, 2 mg/mL in 1× PBS; Click-iT™ EdU Cell Proliferation Kit for Imaging, Alexa Fluor™ 488 dye, Invitrogen, #C10337) 2 h prior to euthanasia. Adult P90 mice were injected with 400 μg EdU via intraperitoneal (i.p.) injections, while P5 and P14 mice were injected with 100 µg EdU via i.p. injections.

The dissected right adrenal glands were fixed in 4% paraformaldehyde (Histolab Products AB, #02178) at +4°C for 24 h. After washing with 1× PBS, they were submerged into 10% and 30% sucrose (Merck KGaA, #27480.294) in 1× PBS for cryoprotection for 24–48 h. Afterwards, the adrenal glands were embedded in O.C.T. (Optimal Cutting Temperature; VWR Chemicals, #361603E) and frozen on dry ice. The frozen blocks were stored at –80°C until cryosection

was performed. Cryosections of 10 µm were collected on Superfrost PLUS glass tissue slides (Epredia, #J1800AMNZ).

Mouse tissue preparation

P1 animals were anesthetized by i.p. injection of 50 µL pentobarbital sodium (60 mg/mL; APL, #338372) per mouse, and perfused with PBS (Merck, #524650). Kidneys, adrenal glands and organ of Zuckerkandl were dissected out as one compact piece and fixed in 4% paraformaldehyde (PFA; Histolab Products AB, #02178) at +4°C overnight, with continuous shaking.

Human tissue preparation

Deep-frozen samples were transferred into ice-cold 4% PFA and fixed at +4°C overnight. The tissue was then processed and embedded in paraffin (Merck, #1.15161), sectioned to 4–5 µm thick sections using HM355S automated microtome (Epredia, #905200) with microtome blades MX35 Ultra (Epredia, #3053835), and dried to Superfrost PLUS glass tissue slides (Epredia, #J1800AMNZ). Alternatively, deep-frozen, fixed samples were embedded in O.C.T. (VWR, #361603E) and sectioned to 10 µm thick sections using Cryotome (CryoStar NX70, Thermo Fisher Scientific).

Immunofluorescence, Hematoxylin and eosin (H&E) staining and Statistical analyses

The tissues were incubated in blocking buffer with 5% donkey serum (Merck, S30-M) in PBS-T (0.1% Triton X-100; Sigma-Aldrich, #T8787) for 1 h. The tissues were then incubated with

primary antibodies diluted in blocking buffer overnight, at +4°C. The antibodies used: chromogranin B (1:500; Atlas Antibodies, #HPA008759), chromogranin B (1:500; Synaptic Systems, #259 103), tyrosine hydroxylase (1:1000; Novus Biologicals, #NB300-110), tyrosine hydroxylase (1:5000; Immunostar, #22914), SOX2 (1:1000; Seven Hills Bioreagents, #WRAB-1236), SOX10 (1:500; R&D Systems, #AF2864), PHOX2B (1:100; R&D Systems, AF4940), PHOX2B (1:50; Santa Cruz, #376997), NEFM (1:300; Abcam, #ab7794) GFP (1:500, Abcam, #ab13970), SDHB (1:200; Proteintech, #67600-1-Ig). After washing the slides 33× in PBS-T, they were incubated with secondary AlexaFluor-conjugated antibodies at room temperature for 1h in dark. The secondary antibodies used: donkey anti-rabbit AF-555 (#A31572), donkey anti-mouse AF-488 (#A21202), donkey anti-mouse AF-647 (#A31571), donkey anti-goat AF-647 (#A21447), donkey anti-goat AF-488 (#A11055), donkey anti-chicken AF-488 (#A78948), donkey anti-sheep AF-488 (#A11015) donkey anti-sheep AF-555 (#A21436) (all Invitrogen). The tissues were counterstained with 1 µg/mL DAPI (ThermoFisher Scientific, #D3571), incubated with TrueBlack Lipofuscin Autofluorescence Quencher (1:20 in 70% ethanol; Biotium, #23007) for 30s, and thoroughly washed in PBS. The coverslips were mounted to the slides with ProLong™ Gold Antifade Mountant with DNA Stain DAPI (Invitrogen, #P36935) and allowed to dry. The images were acquired with ZEISS LSM980-Airy (alternatively, ZEISS LSM800) confocal microscope (Axio Observer Z1/7) and ZEISS ZEN Blue Microscopy acquisition software, v3.2. Quantification was performed semi-manually using QuPath analysis software v0.4.4 (Bankhead et al., 2017) and graphs were created using GraphPad PRISM, v10 for Mac, (GraphPad Software). Statistical analyses were performed using GraphPad Prism version 10.3.1 for macOS (GraphPad Software, La Jolla California USA). For the positive cell

co-expression analysis, statistical significance was assessed using the non-parametric Kruskal-Wallis test followed by a post hoc Dunn's multiple comparison test. For comparison between adrenal glands and organ of Zuckerkandl, non-parametric Mann-Whitney U test was used. For all data sets, the arithmetic mean ± s.e.m. is reported. P values < 0.05 were considered statistically significant.

For H&E staining, the tissue sections were deparaffinized in xylene (HistoLab Products AB, #02070) and rehydrated using a series of ethanol (Solveco, Sweden) and distilled water washes. When H&E staining was performed on tissues that were previously immunofluorescently labelled, the slides were immersed in PBS and incubated until the cover slips detached. Afterwards, they were incubated in hematoxylin (HistoLab Products AB, #01820) for 5 min followed by a thorough wash in tap water. The slides were then incubated in eosin (HistoLab Products AB, #01650) for 45s, dehydrated in 100% ethanol and xylene, and coverslips were mounted with VectaMount Mounting Medium (Vector Laboratories, #H-5000). The images were acquired with ZEISS Axio Scan.Z1 Slide Scanner and ZEISS ZEN Blue Microscopy acquisition software, v3.1.

Mouse tissue single-cell sequencing, data pre-processing and quality control

For single-cell suspension preparation for single-cell RNA sequencing, multiple adrenal glands from pups within one litter were pooled in 1 mL LBSS (154 mM NaCl, 5 mM KCl, 3.6 mM $NaHCO_3$, 5 mM HEPES, 11 mM glucose) on ice after cutting them open to expose the medulla. The cortex from adrenal glands of mice older than 13 days was partially peeled off to enrich for medullary cells.

After LBSS was exchanged three times, the tissues were incubated in 500 µL pre-warmed papain solution (25 U/mL) in dissociation medium (DMEM/F12 medium without dye, with HEPES buffer, 1 mM L-Cysteine, 1 mM $CaCl_2$ and 1 mM EDTA) for 30 min at 37°C. Afterwards, the medium was replaced three times by 1 mL trituration buffer (DMEM/F12 medium without dye, with HEPES buffer, 2% horse serum, 1 mM $CaCl_2$, 1 mM EDTA) and eventually by 500 µL trituration medium and 12.5 µL RNasin® Plus Ribonuclease Inhibitor (Promega, Cat No. N2615) and triturated gently twenty times with 3 fire-polished Pasteur pipettes of decreasing diameters. Subsequently, the cell suspension was filtered through a 40 µm strainer, and YFP positive single cells were sorted into 384 well-plates prefilled with Smart-seq2 lysis buffer. The well-plates were then sealed and packaged with dry ice immediately and transferred to the Eukaryotic Single Cell Genomics (ESCG) facility at SciLifeLab for further processing.

Mouse single-cell data clustering and cell type identification

Gene expression of cells was log normalized, standardized and scaled using NormalizeData() and ScaleData(). Cell cycle score was calculated for each and all cells using G2M and S gene sets provided with the package and as prevoiusly described [1]. We adjusted gene expression by the effect of cell cycle, mitochondrial expression, and library size. We identified highly variable genes with FindVariableFeatures() using nfeatures = 2500. We then clustered the data with FindClusters() using resolution=0.6. The mutual nearest neighbors were calculated using FindNeighbors() with dims=40 principal components and k.param =2 0 neighbors. We then identified *Sox2*$^+$ cells in glial clusters 6 (corresponding to E17 cells) and 11 (corresponding to P5, P14, P90, and aged cells) as cells showing standardized gene expression larger than 0.

Cell clusters identified in the single-cell dataset were annotated based on the known cell type marker genes [2].

Specific differential expressed genes and GO term pathway enrichment analysis

To identify specific DEGs in mouse embryonic and postnatal glia cells, we conducted differential expression analysis by comparing each cellular cluster against another cluster in a pairwise manner. We used the "FindMarkers()" function from the Seurat R package [3] for this analysis, considering genes with adjusted *P* values below 0.05 and log fold change above 0.5 as significant DEGs. To identify specific DEGs, we took the intersection of upregulated DEG lists from all pairwise comparisons involving a given cluster. Genes present in the final intersections were classified as specific DEGs for that cluster.

Gene-ontology enrichment analysis was performed using the ClusterProfiler R package (https://doi.org/10.1089/omi.2011.0118). Specifically, we applied the "enrichGO()" function using the selected gene list as inputs. Multiple testing correction was conducted using the Benjamini-and-Hochberg (BH) method with significant enriched GO terms selected based on adjusted *P* values below 0.05. We used 'org.Mm.eg.db' database for genome-wide annotation for the mouse genome.

Cellular interaction network

We inferred cell-cell-communication network using the CellChat R package [4] for each age in this study. Specifically, we performed two parallel analysis using wild-type mouse data. (a) Global Cell Type Interactions: Cell types comprising at least 10 cells in each age group were analyzed (Fig. 5G and 5H, Suppl. Fig. S5E, S5G, S5H, and S5J). (b) Subgroup-Specific Interactions: We focused on ADR chromaffin cells, NOR chromaffin cells, and glial cells in each age group (Fig. 5I).

Human single-nuclei data pre-processing and quality control

Human single-nuclei raw sequencing data were hard-clipped to remove adapters and reads shorter than 20 bases with TrimGalore v0.6.1. FastQC v0.11.8 (https://www.bioinformatics.babraham.ac.uk/projects/fastqc) was used to further remove low quality reads, such that reads failing 3 or more of the tests were excluded. After quality control, the remaining high-quality reads were aligned to the human transcriptome (hg38, GRCh38.p13) with STAR v2.7.11a. Transcripts were counted and gene length-normalized to transcripts per million (TPM) with RSEM v1.1.3 [5] with standard parameters in single-cell mode (--single-cell-prior). Cells underwent quality control by using cutoffs of at least 1,000 genes/cell and a mitochondrial fraction <30%, 523 (~15%) low-quality cells were filtered out. For all downstream analyses, TPM matrices were taken from only the cells relevant to the analysis, log2((TPM/10)+1)-transformed as in [6], and only genes with an average expression of >4.5 log2(TPM) across all cells in the matrix were kept. Thereafter, gene expression levels per cell were mean-centered by the average expression of each gene.

Human single-nuclei data clustering and cell type assignment were performed as followed: A matrix of 7,464 genes x 2,895 cells was created as per above from all cells passing initial QC. Thereafter, the matrix underwent UMAP dimensionality reduction and DBscan clustering (minpts=10). Each cluster was roughly assigned an initial cluster type based on the top 50 differentially expressed genes in that cluster compared to all other cells (Table S6).

Since our dataset was heavily enriched in neuroendocrine cells, impacting the clustering of other cell types, all non-neuroendocrine cells were then separately clustered to accurately assign microenvironment cell type (Table S7). Upon this second clustering, 111 cells were removed due to

forming patient-specific clusters with mixed neuroendocrine-immune signatures, indicating doublet formation. FACS analysis also confirmed that these samples were enriched in S phase – increasing the risk of doublet formation due to uptake of PI stain. Finally, performing CNA analysis on these cells showed weaker CNA patterns plus a 6p amplification, typical of immune cells due to the HLA locus, in cells assigned as doublets (data not shown). Additionally, a group of 198 TME cells, having few differentially expressed genes and significantly enriched in noncoding genes to other cells (35% vs 20%, $p<2.2E-16$, t-test), was removed as low-quality cells.

Copy number aberration (CNA) inference

For each patient, this reference was added to all neuroendocrine and Schwann cells from that patient to create a new matrix, which was filtered and centered as earlier described. For reanalysis of the Zethoven et al. dataset [7], adrenocortical, chromaffin, endothelial cells and fibroblasts from the same patient, as well as all SCLCs from two normal adrenal medulla samples were instead used as reference. Genes were reordered by chromosomal location and normalized expression values were limited to –3 and 3. For each cell, a moving 100-gene average was calculated at each chromosomal position, giving initial CNA values.

For each of the three reference cell types, a mean CNA value was taken, averaging the moving averages across all cells from that type. To infer relative copy number changes compared to cells with a normal karyotype, the highest of these three values was then subtracted from all positive CNA values and the lowest was subtracted from all negative values. Additionally, all values between –0.15 and 0.15 were assumed to reflect noise and set to zero.

To infer genetic subclones, the top 2/3 of the CNA matrix by absolute value of the CNA signal underwent UMAP dimension reduction and overclustering using graph-based Louvain clustering (k=15). An average CNA value per cluster per chromosome arm was then calculated and deletion/amplification was defined by average CNA value < –0.15 or >0.15, respectively. Clusters were then merged if their deletion/amplification events were the same across all chromosome arms. This was repeated, and new average CNA values calculated, until the remaining clusters differed by at least one chromosome arm.

Neoplastic cell definitions

To stringently define malignant cells, we used CNA signal and CNA correlation as quantitative metrics. CNA signal was defined as mean of CNA absolute values across the top 20% genes by CNA absolute value. Then, for each cell, a correlation coefficient, called CNA correlation, was calculated between the CNA values of that cell and the average CNA profile of the top 20% cells by CNA signal. Cutoffs for each metric were set at median +2SD of the reference cells, and only cells passing both cutoffs were classified as malignant (Suppl. Fig. S5B).

Supplementary References

1. Kowalczyk, M.S., et al., *Single-cell RNA-seq reveals changes in cell cycle and differentiation programs upon aging of hematopoietic stem cells.* Genome Res, 2015. **25**(12): p. 1860-72.
2. Bedoya-Reina, O.C., et al., *Single-nuclei transcriptomes from human adrenal gland reveal distinct cellular identities of low and high-risk neuroblastoma tumors.* Nat Commun, 2021. **12**(1): p. 5309.
3. Satija, R., et al., *Spatial reconstruction of single-cell gene expression data.* Nat Biotechnol, 2015. **33**(5): p. 495-502.
4. Jin, S., et al., *Inference and analysis of cell-cell communication using CellChat.* Nat Commun, 2021. **12**(1): p. 1088.
5. Li, B. and C.N. Dewey, *RSEM: accurate transcript quantification from RNA-Seq data with or without a reference genome.* BMC Bioinformatics, 2011. **12**: p. 323.
6. Puram, S.V., et al., *Single-Cell Transcriptomic Analysis of Primary and Metastatic Tumor Ecosystems in Head and Neck Cancer.* Cell, 2017. **171**(7): p. 1611-1624 e24.
7. Zethoven, M., et al., *Single-nuclei and bulk-tissue gene-expression analysis of pheochromocytoma and paraganglioma links disease subtypes with tumor microenvironment.* Nat Commun, 2022. **13**(1): p. 6262.

Supplementary Figure Legends

Supplementary Figure Legends

Suppl. Fig. S1

(A) Immunofluorescence and H&E staining of mouse adult adrenal gland showing adrenal medullary glial cells co-expressing SOX2 and SOX10. Scale bars in the adrenal glands and insets are 200µm and 10µm, respectively.

Suppl. Fig. S2

(A) Representative image showing immunofluorescence staining for CHGB, PHOX2B and NEFM in adrenal gland and organ of Zuckerkandl of P1 mice. Scale bars and insets are 100µm and 20µm, respectively. **(B)** Representative image showing immunofluorescence staining for SOX2, PHOX2B and SOX10 in adrenal gland and OZ of P1 mice. Scale bars and insets are 100µm and 20µm, respectively. **(C)** Representative image showing immunofluorescence staining for SOX2, TH and SOX10 in adrenal gland and organ of Zuckerkandl of P1 mice. Scale bars and insets are 100µm and 20µm, respectively. **(D)** Representative image showing immunofluorescence staining for SOX2, TH and PHOX2B in adrenal gland and OZ of P1 mice. Scale bars and insets are 100µm and 20µm, respectively.

Suppl. Fig. S3

(A) Representative image showing immunofluorescence staining for CHGB, TH and PHOX2B in 20-week-old human adrenal gland. The medullary region is indicated by dash line. Scale bars in the adrenal gland and insets are 100 µm and 20 µm, respectively.

Suppl. Fig. S4

(A) UMAP plot showing sample identities of scRNA-Seq data of mouse adrenal tissue. **(B)** UMAP plot illustrating the detailed age grouping of cells from the mouse adrenal gland. **(C)** UMAP plot displaying cellular clusters identified in the scRNA-Seq data of mouse adrenal tissue. **(D)** Dot plot showing the expression patterns of cell type-specific marker genes across identified clusters in the scRNA-Seq dataset. **(E)** Heatmaps representing the relative centrality of each aged mouse adrenal gland cell group within the NOTCH signaling networks, assessed via four network centrality measures (sender, receiver, mediator, influencer). **(F,G)** UMAP plot illustrating the expression of Dlk1 and NOTCH1. **(H)** Network diagram showing inferred Dlk1-Notch1 ligand-receptor interactions among cell types in P5 and P14 mouse cells. **(I)** Network diagram showing inferred Dlk1-Notch1 ligand-receptor interactions among cell types in E17 mouse cells. **(J)** UMAP plot illustrating the expression of Wnt6, Lgr5, Sfrp1, and Sfrp5. **(K)** Network diagram showing inferred Wnt6 - (Fzd3 + Lpr5/6) ligand-receptor interactions among cell types in postnatal mouse cells.

Suppl. Fig. S5

(A) UMAP of 2,586 single nuclei colored by sample of origin. **(B)** Malignant cell definition: Example from sample 198. The y-axis represents CNA signal and the x-axis CNA correlation (see Methods). Each point is a cell, colored by assigned cell type. Lines represent cutoffs (median + 2SD of adrenocortical,

fibroblast and endothelial cells). Only cells passing both cutoffs were defined as malignant. **(C) CNA metrics for SOX2^{+}SOX10^{+}** neoplastic **cells.** Boxplots showing CNA signal and CNA correlation for neuroendocrine cells, split by SOX2/SOX10 expression, Schwann cells and stroma (all fibroblasts, endothelial and adrenocortical cells). **(D)** Recurrently differentially expressed genes in PPGL #264**.** Rows are genes significantly over/under expressed in all paired comparisons between malignant cells from sample #264 and each other tumor sample. Columns are mean expression values of each gene per sample. All values were centered by the mean expression in sample #264.

Supplementary Table Legends

Suppl. Table S1. Specific up-regulated differentially expressed gene list from scRNA-Seq data **of mouse adrenal gland clusters defined in Fig. 5A** $(P.adj < 0.05)$**.** P-values are adjusted using Bonferroni correction (as detailed in Methods).

Suppl. Table S2. Mouse postnatal glia enriched gene ontology (GO) terms shown in Fig. 5F $(P.adj < 0.05)$**.** Postnatal glia specific differentially expressed gene (as defined in Table S1) were used as input for GO analysis. P-values are adjusted using Benjamini-and-Hochberg (BH) methods (as detailed in Methods).

Suppl. Table S3. List of PPGL samples and corresponding mutation status from Fig. 6 and S5. MUT = Mutant. WT = Wild type. Const = constitutive.

Suppl. Table S4. Genes significantly up- or downregulated in all pairwise comparisons of PPGL sample 264 versus every other sample.

Suppl. Table S5. Differentially expressed genes between malignant and nonmalignant glia (refererred as Schwann cell like cells, SCLCs) as prevously defined in Zethoven et al. dataset [7].

Suppl. Table S6. Top 50 differentially expressed genes per cluster across all cells defined in Figure 6A.

Suppl. Table S7. Top 50 differentially expressed genes per cluster in the tumor microenvironment (TME).

Suppl. Figure S1

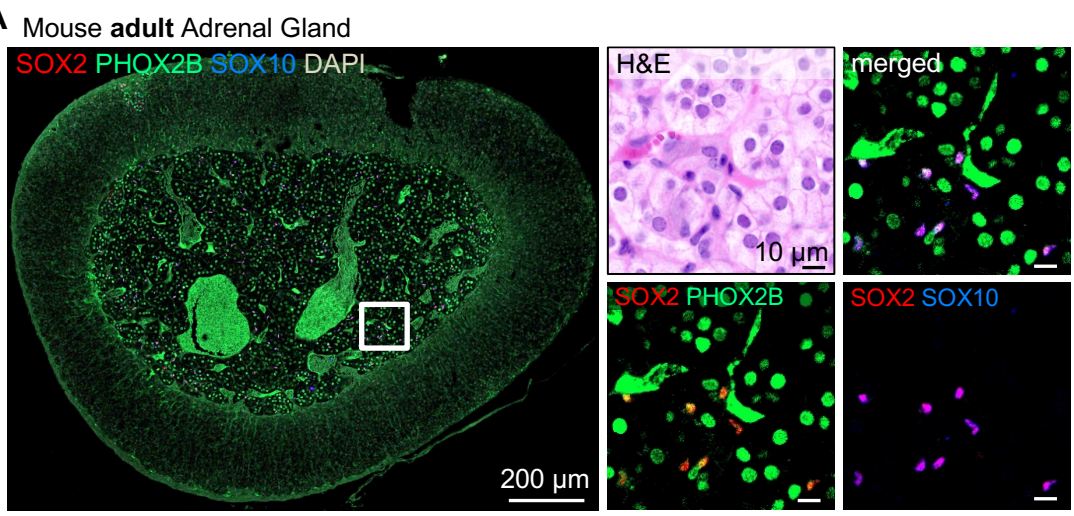

Suppl. Figure S2

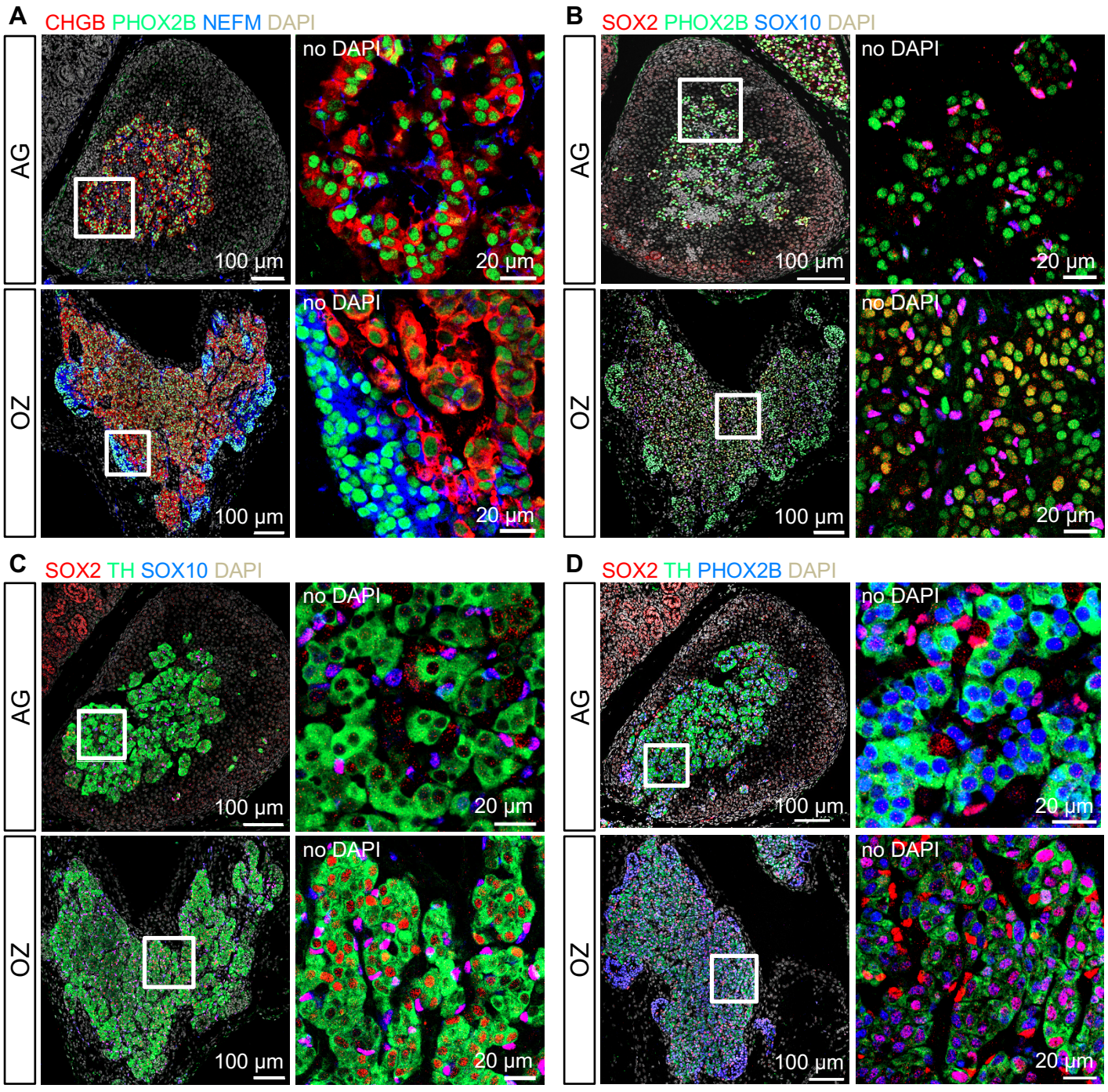

Suppl. Figure S3

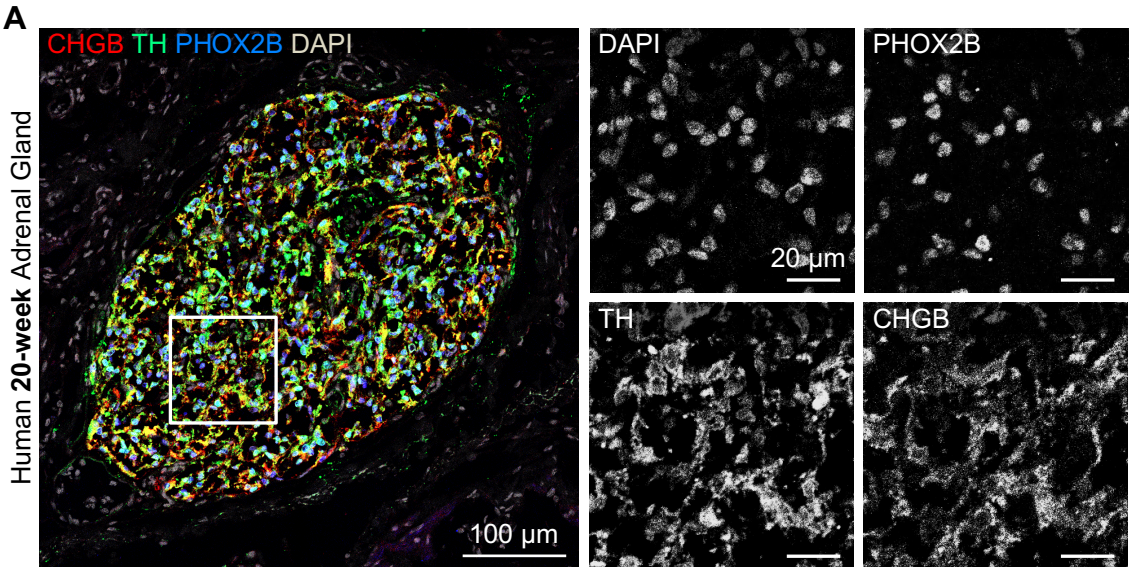

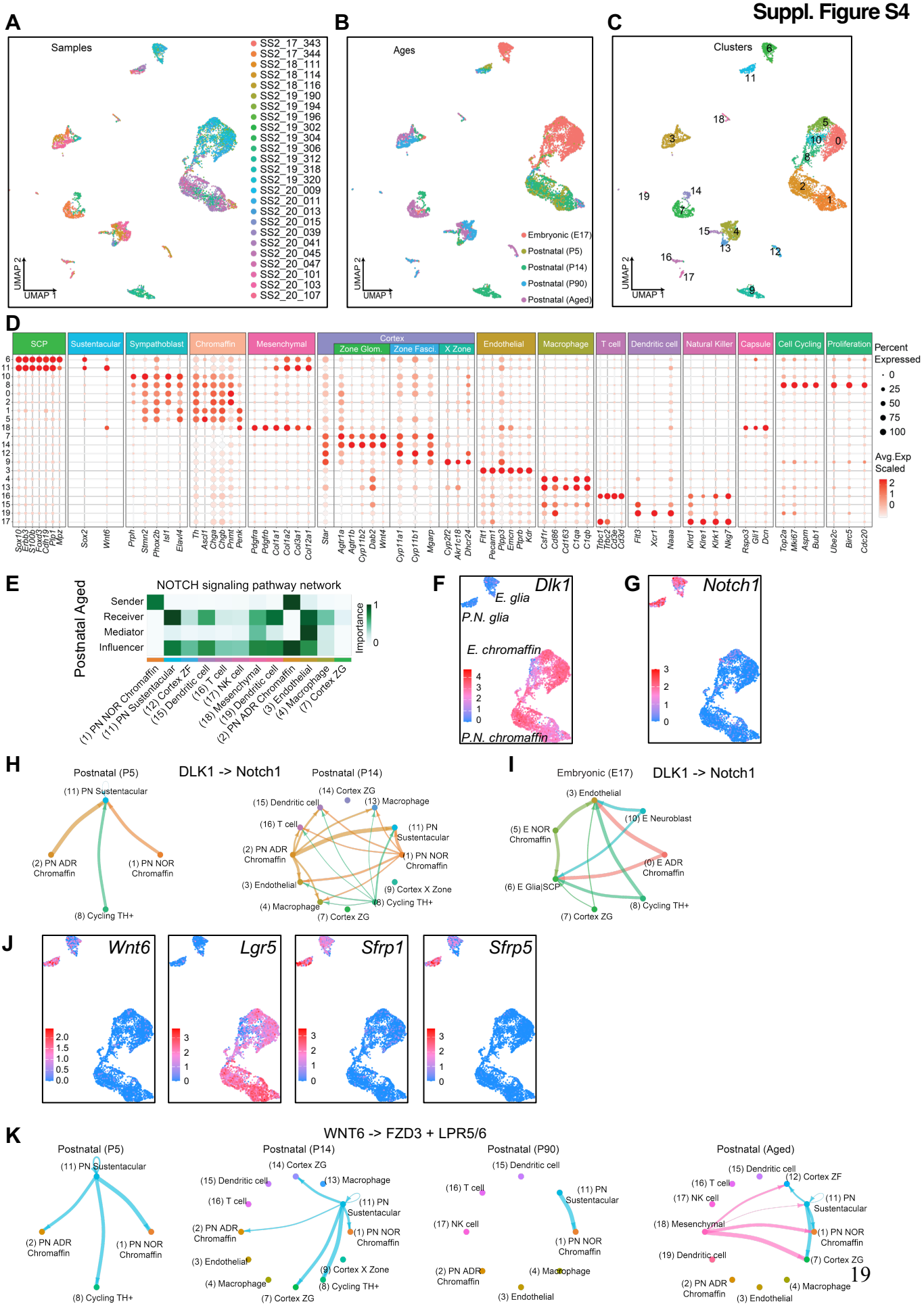
A
Samples
B
Ages
C
Clusters
D
SCP
Sustentacular
Sympathoblast
Chromaffin
Mesenchymal
Cortex
Zone Glom.
Zone Fasci.
X Zone
Endothelial
Macrophage
T cell
Dendritic cell
Natural Killer
Capsule
Cell Cycling
Proliferation
Percent Expressed
Avg.Exp Scaled
E
NOTCH signaling pathway network
Postnatal Aged
Sender
Receiver
Mediator
Influencer
Importance
F
Dlk1
E. glia
P.N. glia
E. chromaffin
P.N. chromaffin
G
Notch1
H
Postnatal (P5)
DLK1 -> Notch1
Postnatal (P14)
I
Embryonic (E17)
DLK1 -> Notch1
J
Wnt6
Lgr5
Sfrp1
Sfrp5
K
WNT6 -> FZD3 + LPR5/6
Postnatal (P5)
Postnatal (P14)
Postnatal (P90)
Postnatal (Aged)

Suppl. Figure S5